INTERPLAY BETWEEN SINGLE-PARTICLE AND COLLECTIVE DEGREES OF FREEDOM IN THE EXCITATION OF THE LOW-LYING QUADRUPOLE STATES IN ^{142}Nd

R.K J SANDOR [a], H P BLOK [a], U GARG [a,b], M N.HARAKEH [a], C W DE JAGER [c], V Yu PONOMAREV [d], A I VDOVIN [d] and H DE VRIES [c]

[a] *Natuurkundig Laboratorium, Vrije Universiteit, P O Box 7161, NL-1007 MC Amsterdam, The Netherlands*

[b] *Physics Department, University of Notre Dame, Notre Dame, IN 46556, USA*

[c] *National Instituut for Kernfysica en Hoge-Energie-Fysica, sectie K, P O Box 41882, NL-1009 DB Amsterdam, The Netherlands*

[d] *Laboratory of Theoretical Physics, Joint Institute for Nuclear Research, Dubna, Head post office P O Box 79, SU-101000 Moscow, USSR*

Received 16 August 1989

The low-lying quadrupole states in ^{142}Nd were investigated by inelastic electron scattering The momentum transfer range covered was 0 5–2 8 fm^{-1} The extracted transition charge densities indicate quite different characters for these states On the basis of a quasiparticle–phonon nuclear model calculation this difference can be understood as arising from an interplay between collective and single-particle aspects

Electron scattering is well suited to investigate the spatial properties of the nuclear wave function due to the well understood relationship between the measured cross section and the nuclear charge and current densities. Shape differences in these densities make it possible to discriminate between collective and non-collective modes of excitation for transitions of the same multipolarity Effort has been spent already to disentangle the contributions of both degrees of freedom in for instance ^{88}Sr, ^{89}Y and ^{90}Zr by Schwentker et al. [1] and in the even Zn isotopes by Neuhausen et al [2] For heavier nuclei this proves to be much more difficult, since the high level density at increasing excitation energies makes it practically impossible to resolve most of the states The introduction of the second generation electron accelerators with a much improved energy resolution, $\Delta E/E \leqslant 10^{-4}$, has given the opportunity to extract transition densities at higher excitation energies with better accuracy Results will be presented here on three of the lowest four quadrupole states in ^{142}Nd, a semimagic nucleus with a closed neutron shell The extracted transition charge densities, which display collective as well as single-particle features, are compared with results of the quasiparticle–phonon model (QPM), a model which has successfully described excitations over a wide range of nuclei Detailed information about different aspects of the QPM can be found in refs [3–5]

The data were taken at the NIKHEF-K facility [6] with the magnetic QDD spectrometer In order to be able to resolve the different states at excitation energies up to 4 MeV the best possible resolution was needed The intrinsic system resolution is $\Delta p/p \leqslant 10^{-4}$, but by means of software corrections (ray tracing algorithms) [7] one is able to improve on this up to 7×10^{-5}, resulting for this experiment in an energy resolution ranging from 12 keV for the lowest incident electron energy (112 MeV) up to 30 keV for the highest (450 MeV) The scattering angle ranged from 36° to 83°, corresponding to effective momentum transfers $q_{\text{eff}} = q(1 + 1\ 33 Z\alpha\hbar c/EA^{1/3})$ between 0.5 and 2 8 fm^{-1} One additional measurement at a backward angle of 154° and an energy of 80 MeV was performed to investigate the transverse contribution to the form factor This q-range is large enough to permit the determination of the ground state charge and the transition charge densities throughout the nucleus The spectrometer acceptance solid angle varied from 0 35 to 5 6 msr The overall efficiency of

0370-2693/89/$ 03 50

the detection system was checked before each measurement by a short run on the elastic and inelastic scattering to the first excited state of ^{12}C, and was always found to be larger than 98% The collected charge was measured with a toroid monitor with an accuracy of 0.1% The target was a thin foil of 99% isotopically enriched ^{142}Nd with a nominal thickness of 10 mg/cm^2. For optimum resolution the target angle was set in transmission mode Most of the data were taken in event-by-event mode, to allow off-line software corrections for kinematical broadening and spectrometer aberrations For the smallest q-values this was not possible due to the high count rates and therefore data were acquired on line in spectral form However, since these low-q measurements were made at forward angles with a small solid angle of 0 35 msr, the loss in resolution due to the kinematical broadening and spectrometer aberrations was negligible

Cross sections were extracted from the measured spectra by a line-shape fitting technique with the program ALLFIT [8], which corrects for straggling, bremsstrahlung and Schwinger effects Uncertainties due to detector efficiencies, target alignment and solid angle were corrected for by the aforementioned efficiency calibration runs on ^{12}C. Furthermore, the ratio of the cross sections for the ground state of ^{12}C and the first excited 2^+ state, both of which are known very accurately as a function of momentum transfer [9,10], determines the exact beam energy, in the momentum transfer region above 2 15 fm^{-1} within an error of 0 5% For the momentum transfers below 2 15 fm^{-1} the usual method of energy calibration by recoil differences was used The only uncertainties remaining were the unknown target thickness and uniformity Correction for these was made in the following way the target thickness was determined by a fit to the elastic form factor data with a free overall normalisation Remaining fluctuations in the order of 3% or less in the individual elastic cross sections were ascribed to the non-uniformity of the target All inelastic cross section data were corrected with these factors In fig. 1 the resulting form factor data are shown for the 2_1^+, the 2_2^+ and the 2_4^+ states The level at 2 550 MeV is a candidate [11] for the 2_3^+ state, but its cross section turned out to be too small to be observed in the present experiment. As can be concluded from fig. 1 the structure of the 2_2^+ state deviates considerably from that of the 2_1^+ and 2_4^+ states, since the second form factor maximum lies at a higher transferred momentum (1.3 fm^{-1} versus 1 1. fm^{-1})

The DWBA code FOUBES [12] was employed to extract the transition charge densities These densities were parametrized using the Fourier–Bessel series

$$\rho_\lambda(r) = \sum_{\mu=1} A_\mu q_\mu^{(\lambda-1)} j_\lambda(q_\mu^{(\lambda-1)} r), \quad r < R_c,$$

$$\rho_\lambda(r) = 0, \qquad r > R_c, \qquad (1)$$

where $q_\mu^{(\lambda-1)} R_c$ is the μth zero of the spherical Bessel function $j_{\lambda-1}(x)$ and R_c is a cutoff radius, beyond which $\rho_\lambda(r)$ is so small that it can be neglected. The transition current $J_{\lambda,\lambda+1}$ was neglected in the analysis, which seems a reasonable assumption in the light of the relatively forward scattering angle, which never exceeded 83°, and the expected small contribution of the transverse form factor This assumption is confirmed by the analysis of the transverse datapoint at 80 MeV and 154°, where the transverse components of the cross section for the quadrupole status turn out to be less than 3% of the longitudinal ones In order to eliminate unphysical oscillations in the transition charge densities at large radii, a so-called tail bias [13] was applied. To account for the limited q-range measured, a high-q constraint was used to determine the incompleteness error. For the first and second 2^+ states values for the reduced transition probability $B(E2)$ as known from the literature [14] were added as data points The relation between $B(E\lambda)$ and the transition charge density for a transition from a 0^+ state to a natural parity state with spin λ is

$$B(E\lambda) = (2\lambda+1)\left|\int_0^\infty \rho_\lambda(r) r^{2+\lambda}\, dr\right|^2 \qquad (2)$$

This data point basically determines the form factor at the photon point

The extracted transition charge densities [#1] are shown in fig 2 with error bands indicating the uncertainties with which these transition densities are determined It is clear from this figure that these tran-

[#1] Experimental transition densities in the form of tables of Fourier–Bessel coefficients can be obtained upon request from R K J Sandor

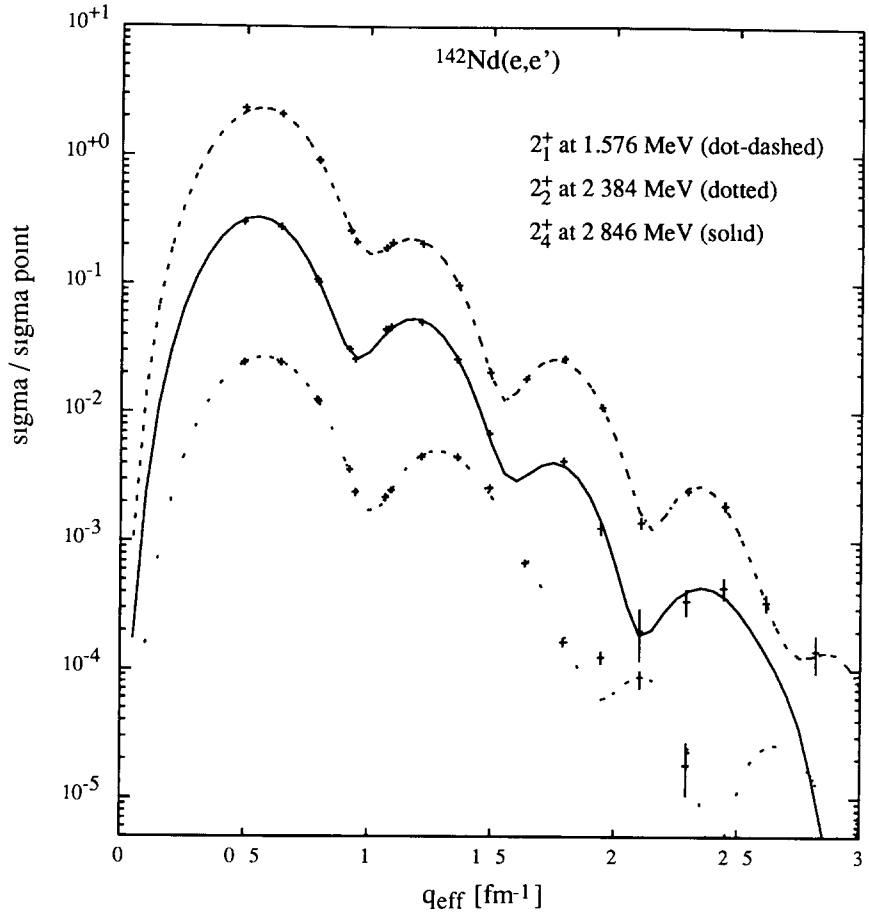

Fig 1 The inelastic form factor data for 2^+ states in ^{142}Nd from the present experiment The curves represent fits to the first excited 2^+ state (dot-dashed) at 1 576 MeV, the second (dotted) at 2 384 MeV and the fourth (solid) at 2 846 MeV, respectively For plotting purposes the form factor data and the fit for the second 2^+ state have been divided by 10

sition densities display very different characters For instance, whereas the transition densities of the 2_1^+ and the 2_4^+ states peak at the nuclear surface ($\sim$5 7 fm) as expected for collective states, that for the 2_2^+ state peaks more inward at $\sim$5 1 fm with a pronounced negative lobe in the nuclear interior In order to understand these different characters displayed by the quadrupole transition charge densities in ^{142}Nd, calculations were performed in the framework of the QPM

The QPM is an microscopic nuclear model in which the interplay between collective and single-particle degrees of freedom is taken into account by performing the calculations in two steps First, basis states called phonons, are generated whereby phonons are defined as (both collective and non-collective) solutions of the BCS quasiparticle RPA equations [15] Second, two-phonon states are constructed and the coupling between the one- and two-phonon states is included This approach thus accounts for pairing as well as multipole correlations.

The computational procedure is as follows First, the single-particle states are calculated in a Saxon–Woods (SW) potential including a spin–orbit term The parameters used for the SW potential are $V=-57\,7$ MeV, $r_0=1\,24$ fm, $a=0.63$ fm, $V_{so}=10\,0$ MeV [16] RPA calculations are then performed in which all bound states and narrow quasibound states

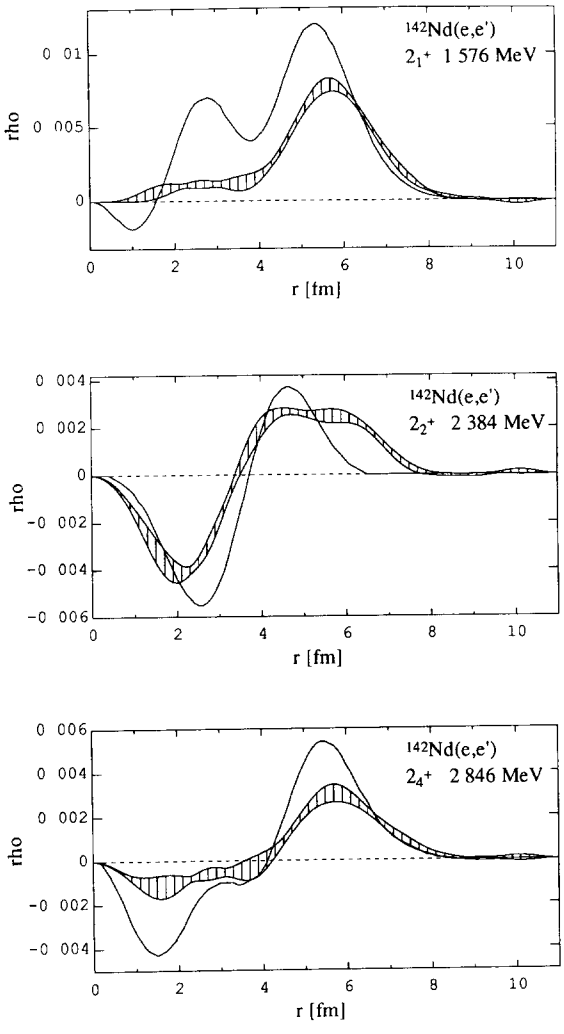

Fig 2 The transition charge densities from experiment (curves with error bands) compared with the theoretical calculations (solid lines) for the three excited quadrupole states at respectively 1 576, 2 384 and 2 846 MeV in ^{152}Nd

with a width, due to the centrifugal and/or Coulomb barrier, less than a few keV are included (i.e. all proton and neutron subshells up to $1j_{15/2}$ and $1i_{11/2}$) Pairing correlations are treated in the BCS approximation, using a schematic pairing force with a standard force strength $G=17/A$ MeV (i.e. 0 12 MeV for ^{142}Nd) This is chosen to match the odd–even mass difference for the $N=82$ isotones. The resulting proton pairing gap is $\Delta p=1.2$ MeV. The phonons are then produced by solving the quasiparticle RPA equations [15], in which schematic particle–hole multipole forces of the form

$$V(1,2)=\sum_{\lambda,\mu,T}\chi_T^{(\lambda)}P_T R(r_1)Y_{\lambda,\mu}(\theta_1,\phi_1)$$
$$\times R(r_2)Y^*_{\lambda,\mu}(\theta_2,\phi_2) \qquad (3)$$

are assumed, where P_T projects out isospin $T=0$ or $T=1$ components The strength ratio for the isoscalar and isovector forces was set at $\chi_1^{(\lambda)}/\chi_0^{(\lambda)}=-1.2$ and the absolute strength for each multipole term, 2^+, 3^-, 4^+, 5^- and 6^+, was adjusted such that the energy of the lowest solution agrees with the experimental energy for the lowest state of that multipolarity The radial functions $R(r)$ in these forces are taken as the derivative of the central part of the SW potential Once the quasiparticle RPA phonons have been determined in this way, the second step of the calculation consists of constructing a basis of two-phonon states Then the coupling between one- and two-phonon states is calculated microscopically [4,5] by diagonalizing the hamiltonian in a basis consisting of the one- and two-phonon states.

The quasiparticle RPA predicts four 2^+ one-phonon states below 4 MeV, which are listed in table 1 No effective charges have been used for the calculation of the $B(E2)$ values, because this is expected to be unnecessary in view of the large single-particle basis used. Since the pairing correlation in the neutron system vanish because of the closed neutron shell, the lowest neutron particle–hole 2^+ configuration has an energy higher than 5 MeV and consequently proton components dominate in the states of table 1 Clearly, the 2_1^+ state has the most collective character. The 2_2^+ and the 2_3^+ states, as expected, have a much smaller $B(E2)$ value. However, the 2_4^+ state is again collective, its $B(E2)$ being only four times smaller than that of the 2_1^+ A possible explanation lies within the subshell structure The two proton subshells $1g_{7/2}$ and $2d_{5/2}$ are close together and close to the Fermi level, whereas other subshells, notably $1h_{11/2}$, $2d_{3/2}$ and $3s_{1/2}$ have about 2 MeV higher single-particle energies. This results in about 1 MeV higher quasiparticle energies as one also observes in the adjacent odd nuclei. The 2_4^+ state is mainly built from configurations involving the latter orbits and therefore it does not lose most of its E2 strength to the collective 2_1^+ state, as the non-collective 2_2^+ and 2_3^+ states do If the transition charge densities for

Table 1
Comparison of experimental and theoretical excitation energies and transition probabilities for the lowest four quadrupole states in ^{152}Nd

i	$\omega(2_i^+)$ [MeV]			$B(E2,\uparrow)[e^2\,fm^4]$		
	experimental	theory		experimental	theory	
		a)	b)		a)	b)
1	1 576	1 70	1 58	2806± 4 [c]	4000	4000
2	2 385	2 44	2 42	230±23 [c]	17	30
3	2 550(?)	2 49	2 46		45	6
4	2 846	3 28	3 07	452±10 [d]	1000	700

[a] Results of RPA calculations for the one-phonon quadrupole states
[b] Results of calculations after mixing between one-phonon and two-phonon states
[c] Ref [14]
[d] Present result

these states are calculated, one sees that for both the 2_1^+ and the 2_4^+ state they are mostly surface peaked, as expected for collective states, whereas the transition charge densities of the 2_2^+ and the 2_3^+ states have a very pronounced volume peak.

After coupling of the one- and two-phonon states one obtains the results listed in table 1 under b) There are 16 two-phonon configurations below 5 MeV The coupling of the one- and two-phonon states is not very strong, as is usual for semi-magic nuclei [17] The first quadrupole $2_1^+ \times 2_1^+$ two-phonon state is located rather high ($E_x = 3\,4$ MeV), whereas other two-phonon states lie still higher ($E_x > 4$ MeV) Therefore, the collective and non-collective one-phonon components dominate in the wave functions of the 2^+-states lower than 3 MeV Indeed the admixtures of the two-phonon components for the lowest four 2^+ states never exceed a few percent As the transition charge densities of the two-phonon states as a rule [18] are small, the contribution of the two-phonon admixtures to the transition charge densities is hardly visible. More important is the mixing of the different one-phonon components and their renormalisation due to the two-phonon part of the wave function as a whole

In fig 2 the calculated transition charge densities for the 2_1^+, 2_2^+ and 2_4^+ states after folding with the proton charge density are plotted (solid curves) and compared with the experimental data. The theoretical and experimental excitation energies and transition probabilities are summarized in table 1

Clearly, the collective one-phonon components dominate the transition charge densities for the 2_1^+ and 2_4^+ states This is not the case for the 2_2^+ and 2_3^+ states, where the coupling with the two-phonon states leads to strong mixing of the second and third one-phonon states As a result the $B(E2, 0_{g.s}^+ \rightarrow 2_2^+)$ increases [17] although it is still about 1 order of magnitude smaller than its experimental value The shape of the experimental transition charge densities is very well reproduced, however For the 2_3^+ state the interference of the one-phonon components is destructive leading to a drastic change in shape of the transition charge density and lowering of the $B(E2, 0_{g.s}^+ \rightarrow 2_3^+)$ value This is probably also the reason that this state is hardly detected in the present experiment Quite remarkable is the measured and predicted high collectivity of the 2_4^+ state. This is an evidence of the gap in the proton single-particle spectrum ($1g_{7/2}$, $2d_{5/2} \leftrightarrow 1h_{11/2}$, $3s_{1/2}$, $2d_{3/2}$).

In general, the agreement between the theoretical calculations and the experiment is quite good A systematic difference though is the evident shift inward by about 0 4 fm of the calculated positions of the surface maxima of the transition charge densities as compared to the experimental ones This might be connected to the smaller values of the radial and diffuseness parameters of the SW well used in the calculations ($r_0 = 1\,24$ fm, $a = 0.63$ fm) than measured in a ^{142}Nd(e, e'p) experiment also NIKHEF-K ($r_0 = 1.31$ fm, $a = 0\,65$ fm) [19]

In conclusion, we have measured inelastic electron

scattering with a high resolution for the lowest three quadrupole excitations in ^{142}Nd. The experimental data cover a momentum transfer range up to $q_{\text{eff}}=2.8$ fm^{-1}, allowing the accurate determination of the transition charge densities These experimental transition charge densities have been compared with the results of a quasiparticle–phonon calculation. The calculation gives a good description of the data. The occurrence of a collective 2_4^+ state reflects that the proton $1g_{7/2}$ and $2d_{5/2}$ subshells are spaced close together and that there is a gap of a few MeV to the next subshells Furthermore, it has been argued that for semi-magic nuclei like ^{152}Nd the two-phonon components in the transition charge densities of low-lying quadrupole states are small and that the structure of the states up to 3 MeV can be explained by a mixing of the collective and non-collective one-phonon states.

We would like to thank Dr K. Allaart for useful discussions. One of the authors (A.I.V) would like to thank the experimental nuclear physics group of the Vrije Universiteit for its hospitality This work is part of the research program of the Foundation for Fundamental Research of Matter (FOM), which is financially supported by the Netherlands' Organization for Scientific Research (NWO).

References

[1] O Schwentker et al , Phys Rev Lett 50 (1983) 15
[2] R Neuhausen, J W Lightbody Jr , S P Fivozinsky and S Penner, Nucl Phys A 263 (1976) 249
[3] V G Soloviev, Theory of complex nuclei (Pergamon, Oxford, 1976)
[4] A I Vdovin and V G Soloviev, Sov J Part Nucl 14 (1983) 99
[5] V V Voronov and V G Soloviev, Sov J Part Nucl 14 (1983) 583
[6] C de Vries et al , Nucl Instrum Methods 223 (1984) 1
[7] H Blok, E A J M Offerman, C W de Jager and H de Vries, Nucl Instrum Methods A 262 (1987) 291
[8] C E Hyde-Wright, Ph D Thesis, MIT (1984), unpublished
[9] L Cardman et al , Phys Lett B 91 (1980) 203
[10] D G Ravenhall et al , Ann Phys 178 (1987) 187
[11] W P Jones et al , Phys Rev C 4 (1971) 580
[12] J H Heisenberg and H P Blok, Annu Rev Nucl Part Sci 33 (1983) 569
[13] J H Heisenberg, Adv Nucl Phys 12 (1981) 61
[14] F R Metzger, Phys Rev C 18 (1978) 1603
[15] M Baranger, Phys. Rev 120 (1960) 957
[16] V Yu Ponomarev, V G Soloview, Ch Stoyanov and A I Vdovin, Nucl Phys A 323 (1979) 446
[17] A I Vdovin and Ch Stoyanov, Bull Acad Sci USSR, Phys Ser 38 (1974) 119
[18] Dao Tien Khoa, I N Kukhtina and V Yu Ponomarev, Sov J Nucl Phys 44 (1986) 585
[19] J B A M Lanen, NIKHEF-K, Amsterdam, private communication